RSC Advances

A novel POMos-based hybrid with penta-coordinated Mo in trigonal bipyramid: structure and an efficient precursor for hydrodesulfurization catalyst

Ji-Lei Liang, Yu-Kun Lu,* Jin-chong Zhao, Xue-Hui Li, Yuan Pan, Meng-Meng Wu, Yun-Qi Liu* and Chen-Guang Liu

State Key Laboratory of Heavy Oil Processing, Key Laboratory of Catalysis, China National Petroleum Corporation (CNPC), China University of Petroleum (East China), Qingdao 266555, P. R. China
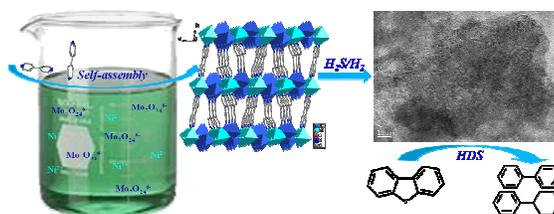
The first POMos-based hybrid with penta-coordinated Mo in trigonal bipyramid for Mo-O clusters;

An efficient precursor for hydrodesulfurization catalyst.

ARTICLE TYPE

A novel POMos-based hybrid with penta-coordinated Mo in trigonal bipyramid: structure and an efficient precursor for hydrodesulfurization catalyst†

Ji-Lei Liang, Yu-Kun Lu,* Jin-chong Zhao, Xue-Hui Li, Yuan Pan, Meng-Meng Wu, Yun-Qi Liu* and
5 **Chen-Guang Liu**

The first POMos-based hybrid with penta-coordinated Mo in
trigonal bipyramid geometry for Mo-O clusters has been
10 **hydrothermally synthesized and characterized by IR, TG,**
XPS, and X-ray diffraction analysis. Structure analysis
indicated penta-coordinated together with tetra-coordinated
Mo existed in the POMos-based hybrid. The hybrid was
successfully used as an efficient precursor for
15 **hydrodesulfurization (HDS) catalyst for the first time.**

Organic-inorganic hybrids have been attracting extensive interest in solid state materials chemistry owing to their unique structural diversities and interesting properties, which make them attractive for applications in catalysis, materials science and 20 electrochemistry.[1] In these fields, polyoxomolybdates (POMos), as one kind of significant Mo-O clusters with controllable shape and excellent property, are outstanding inorganic building blocks for the construction of POMos-based hybrid.[2] As Zubieta indicated that POMos anions can be linked through secondary 25 metal coordination groups forming POMos-based hybrids *via* self-assembly,[3] a variety of novel POMos-based hybrids with $\{Mo_{15}O_{47}\}$,[4] $\{Mo_{10}O_{33}\}$,[5] $\{Mo_9O_{30}\}$,[5] $\{Mo_8O_{26}\}$,[6] $\{Mo_7O_{24}\}$,[6e] $\{Mo_6O_{19}\}$,[7] $\{Mo_5O_{16}\}$,[8] $\{Mo_4O_{14}\}$,[9] $\{Mo_3O_{10}\}$[6c] and $\{Mo_2O_7\}$[10] were synthesized. These works have greatly enriched the 30 polyoxometalates (POMs) chemistry. Among various POMos-based hybrids, molybdenum is commonly tetra- or hex-coordinated, and no hybrid with penta-coordinated molybdenum in a trigonal bipyramid manner is available since it is inherently coordinative unsaturated. As is well known that Ni-Mo-O clusters 35 play an important role in the construction of HDS catalyst for the petroleum refining industry.[11] Inspired by the self-assembly strategy of POMos-based hybrids in POMs chemistry, we selected rational organic ligand to link Ni-Mo-O clusters in impregnating solution and form a new POMos-based hybrid, 40 which can not only enrich the POMs chemistry but also provide ideal precursor to develop more active HDS catalyst. On the basis of the above consideration, an interesting layered POMos-based hybrid, $Ni_2(4,4'\text{-bpy})Mo_4(4,4'\text{-bpy})_2O_{14}$ (**1**) (4,4'-bpy=4,4'-bipyridine) was synthesized from the impregnating solution, in 45 which penta-coordinated Mo1 in trigonal bipyramid and tetra-coordinated Mo2 in tetrahedron were found. To the best of our knowledge, this is the first example of penta-coordinated Mo in

trigonal bipyramid geometry for Mo-O clusters. Moreover, Ni and Mo atoms are inserted in **1** with the Ni/Mo ratio of 0.5, an 50 optimal ratio to prepare HDS catalyst. A preliminary study was carried out to explore the use of **1** as precursor for the HDS catalyst of dibenzothiophene (DBT), a representative sulfur compound in gas oil.

1 was prepared by the hydrothermal method[12] and its crystal 55 structure was solved (Table S1, ESI†). During the preparation, we found that the final product was sensitive to the acidity of the starting reaction solution. The pH of the reaction system was controlled at 5.8 to obtain a pure product, whereas beyond the pH only a little irregularly shaped crystalline fragments were 60 obtained. They were also target products which were confirmed by the powder X-ray diffraction. Changing the amount of reactant, temperature (140-180 ℃), and reaction time (3-6 days) had little influence on the final product, and the hydrothermal synthesis was highly reproducible.

65
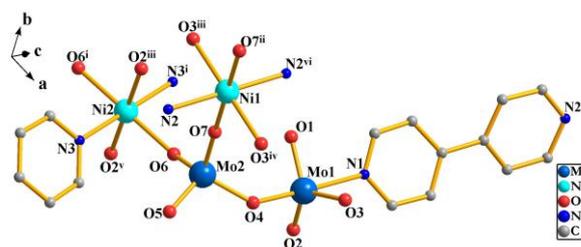
Fig. 1 Asymmetric unit content of 1. Symmetry code: (i) 1-x, -y, -z; (ii) 1-x, -y, 1-z; (iii) -1+x, y, z, (iv) 2-x, -y, 1-z, (v) 2-x, -y, -z, (vi) 3-x, 1-y, 1-z.

Single-crystal X-ray diffraction analysis reveals that **1** consists of two-dimensional Ni-O-Mo bimetallic oxide networks 70 connected by coordination of 4,4'-bpy with Mo and Ni to generate a three-dimensional framework. As shown in Fig. 1, two Ni and two Mo sites exist in the asymmetric unit of **1**, and they are connected by oxygen bridges. In fact, two crystallographic Ni sites both have half occupation of sites. Hence, the ratio of Ni/Mo 75 is 0.5. The hybrid is structurally related to the POMos-based hybrids with dimolybdate $\{Mo_2O_7\}$, but there are some differences. In the available POMos-based hybrids with $\{Mo_2O_7\}$, both of the molybdenum sites are tetra-coordinated in tetrahedron[10b] or hex-coordinated in octahedron.[10a] However, it is 80 noteworthy that the geometry of the Mo1 site in **1** is trigonal

bipyramid, {O(MoO₃)N}, with three oxo groups in the equatorial position and two axial positions occupied by a N atom of 4,4′-bpy and a O of oxo group (Fig. S1, ESI†). The three equatorial bonds make almost perfect trigonal angles with the actual values of 116.2 (l54), 118.0 (152), and 120.5 (156) ° (Table S2, ESI†), and the sum of three angles is 354.7 °. Mo1 atom is displaced by 0.23 Å toward the O from the equatorial plane of the three oxygen atoms (Fig. S2, ESI†). The axial N-Mo-O is slightly bent (177.9 (145) °), with a short Mo-O bond distance of 1.953 (27) Å, and long Mo-N bond distance of 2.314 (37) Å, presumably because of stress imposed by the bridging system.[13] By contrast, the geometry of the Mo2 site is {MoO₄} tetrahedron. To the best of our knowledge, two compounds with penta-coordinated molybdenum were reported by Anderson,[14] however, they were organometallic compounds, and this is the first example of POMos-based hybrid with penta-coordinated molybdenum-oxo cluster in trigonal bipyramid geometry. Besides, The principal axis of the two trigonal bipyramids reported by Anderson is more bent (167.0 °, 169.4 °) than that of **1** (177.9 °), indicating the trigonal bipyramid of **1** is more perfect (Fig. S3, ESI†). The bond valence sum calculations for the Mo atoms (Table S3, ESI†) was calculated by using parameters given by Brown,[15] and the results give the average value 5.96 and 5.93 for Mo1 and Mo2, respectively, indicating that the hybrid contains Mo^{VI} centers. The XPS gives two peaks at 231.7 eV and 234.8 eV ascribed to Mo^{VI} $3d_{5/2}$ and Mo^{VI} $3d_{3/2}$, respectively (Fig. S4, ESI†).[16] All these results further confirm the structure analysis above.

The hex-coordinated Ni in **1** is in a slightly elongated octahedral adduct, {N(NiO₄)N}, of which the axial positions are occupied by two nitrogen donors from two 4,4′-bpy (Ni–N = 2.137(39) Å, N–Ni–N = 180 °). The equatorial plane is defined by two oxygen donors from two {MoO₄} with Ni–O bond distance of 2.084(33) Å and two oxygen donors from two {O(MoO₃)N} with Ni–O bond distance of 2.087(36) Å. The Ni atom is exactly located in the center of the equatorial plane.
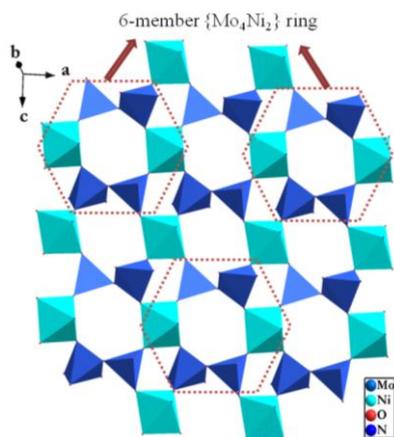
Fig. 2 Two-dimensional layered structure consisting of 6-member {Mo₄Ni₂} rings viewed along the ac plane in polyhedral representation.

As shown in Fig. 2, each {N(NiO₄)N} octahedron can be viewed as an effective junction *via* four oxo groups to link two Mo1 and two Mo2 atoms into a novel two-dimensional layered network. Notably two {MoO₄} tetrahedra, two {N(NiO₄)N} octahedrons and two {O(MoO₃)N} trigonal bipyramids, are linked alternatively in a pattern of corner sharing to form a

unique 6-member {Mo₄Ni₂} ring. Then, the rings are connected to each other *via* corner sharing into a two-dimensional layered network. Finally, the bimetallic layers are connected by 4,4′-bpy, generating a three-dimensional layered structure with the adjacent bimetallic layer distance of 7 Å as shown in Fig. 3. Interestingly, two different coordination modes of 4,4′-bpy are found in Fig. 3. On one hand, some 4,4′-bpys are planar with two N atoms coordinated to Ni sites, forming square channels (11.43×11.40 Å). On the other hand, two pyridine rings of other 4,4′-bpys are twisted with two N atoms coordinated to Ni and Mo, respectively. The square channels are subdivided into three narrow windows due to this coordination mode. For such framework, a 4,4′-bpy coordinating to two different kinds of metal centers is really rare.
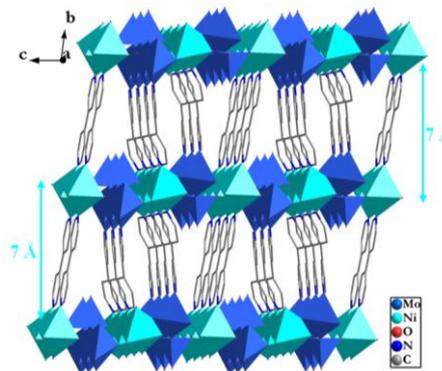
Fig. 3 3-dimentional layered structure of 1 linked by 4,4′-bpy with two different coordination modes of 4,4′-bpy viewed along the ac plane.

As the 4,4′-bpy has a straight and planar structure with a very good π-electron conjugated system, it is favorable for the construction of π···π stacking supported structure.[17] The centroid-to-centriod distances of N2ⁱ- and N1-containing pyridine, N3ⁱᵛ- and N1-containing pyridine are 3.939 and 3.803 Å, respectively, indicating the presence of π···π stacking interactions that further stabilize the crystal structure (Fig. S5, ESI†).

The IR spectrum of **1** (Fig. S6, ESI†) exhibits two bands at 933 and 889 cm⁻¹ which can be attributed to the Mo=O stretching vibrations, while those from 648 to 860 cm⁻¹ are associated to the Mo–O–Mo bending vibrations.[6e] Besides, the bands at 1612, 1538, 1485, 1406 and 1213cm⁻¹ can be regarded as the vibrations of 4,4′-bpy ligands.[18]
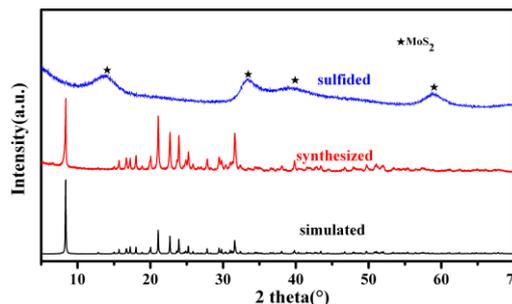
Fig. 4 The sulfided, synthesized and simulated XRD patterns of 1.

The thermal stability of **1** was investigated and the TG curve (Fig. S7, ESI†) shows that it is thermal stable under 360 ℃ and then it begins to decompose, and the total weight loss is 40.53%, corresponding to the release of the 4,4′-bpy ligands, which is in accordance with the calculated value of 39.25% (~1.5 4,4′-bpy),

and the residue should be NiO and MoO_3.

In order to confirm the purity of **1**, the XRD measurement has been performed, as shown in Fig. 4. The result shows that the experimental XRD pattern of **1** is in good agreement with the

5 simulated pattern based on the result from single-crystal X-ray diffraction *via* Mercury 1.4.2 software, indicating that the bulk hybrid is pure. Then the hybrid was sulfided as the catalyst. The XRD pattern of the sulfided hybrid exhibits weak peaks of MoS_2 at 14.1 °, 33.1 °, 39.8 ° and 59.2 °, indicating poorly crystallized

10 structure of the MoS_2 which is the active phase for the HDS catalyst of DBT. It is noted that Ni was incorporated at the edge of MoS_2 and no sulfide of Ni was found.
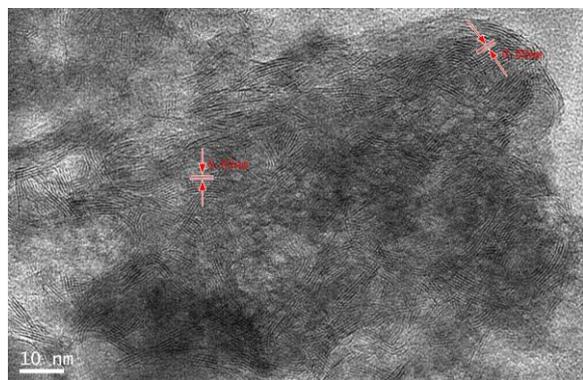
Fig. 5 HRTEM image of the sulfided hybrid.

15 The sulfided hybrid was observed by high-resolution transmission electron microscopy (HRTEM) and the image is presented in Fig. 6. The black fringes correspond to the MoS_2 slabs. These bent fringes presents a spacing of 0.62 nm which is the characteristic of (002) basal planes of MoS_2 crystallite. The

20 fringes appear relatively stacked and disordered, and the number of the stacking layer is about 5-10. Since the hybrid is multi-layered, highly stacking MoS_2 crystallites are formed after sulfidation, which is favored for the preparation of HDS catalyst. The high stacking layer number may mean higher hydrogenation

25 ability of the catalyst.

Table 1 DBT HDS results of the sulfided hybrid.

DBT conversion (%)				$k_{DBT}(10^{-4}$ $g_{cat}^{-1} s^{-1})$	Product selectivity [a] (%)		
1 h	2 h	3 h	4 h		BP	CHB	CHB/BP [b]
22.5	63.2	81.6	92.8	4.4	30.3	58.2	1.9

[a] Determined at about 50 % of total DBT conversion, [b] Obtained by dividing DDS into HYD, DDS= BP; HYD =CHB.

The catalytic results of DBT HDS are shown in Table 1. The DBT conversion can reach 92.8% at 4 h, indicating higher catalytic activity of the catalyst compared to the result reported

30 by Klimova and co-workers.[19] This can also be observed from the value of overall pseudo-first order rate constant k_{DBT} shown in Table 2. There are two pathways in DBT HDS: one is the direct desulfurization (DDS) route to yield biphenyl (BP), and the other is through the hydrogenation (HYD) route to produce cyclo-

35 hexylbenzene (CHB) with tetra-hydrodibenzothiophene and hexa-hydrodibenzothiophene as intermediates.[20] Table 1 also shows the reaction product distributions obtained at 50% of DBT conversion to distinguish the individual contributions of the HYD and DDS routes to the overall HDS performance of the sulfided

40 hybrid. The catalyst showed larger amounts of CHB in comparison with BP and much higher hydrogenation ability, indicating that the catalyst is more favorable for the HYD pathway.

In summary, the first example of POMos-based hybrid with

45 penta-coordinated molybdenum in trigonal bipyramid geometry for Mo-O clusters was hydrothermally synthesized and structurally characterized. More interestingly, penta-coordinated molybdenum together with tetra-coordinated molybdenum exists in the hybrid. Investigation of the catalytic activity property

50 indicated that the hybrid can serve as an efficient HDS catalyst precursor. This work not only enriches the POMs chemistry but also expands the application of POMs in HDS field successfully for the first time. As a continuance of the work, we will investigate the catalytic property of POMs in HDS field in detail.

Notes and references

State Key Laboratory of Heavy Oil Processing, Key Laboratory of
65 *Catalysis, China National Petroleum Corporation (CNPC), China University of Petroleum (East China), Qingdao 266555, P. R. China.*
E-mail: lyk@upc.edu.cn, liuyq@upc.edu.cn

† Electronic Supplementary Information (ESI) available: [Experimental details, instrumentation, crystallographic data, CCDC 943446, diamond
70 pictures, list of bond angle and distance, BVS, TGA, IR, XPS].

1. (a) A. Dolbecq, E. Dumas, C. R. Mayer and P. Mialane, Chem. Rev., 2010, **110**, 6009-6048; (b) P. J. Hagrman, D. Hagrman and J. Zubieta, *Angew. Chem. Int. Ed.,* 1999, **38**, 2638-2684; (c) J. Cao, S. Liu, R. Cao, L. Xie, Y. Ren, C. Gao and L. Xu, *Dalton Trans.,* 2008, 115-
75 120; (d) X. Wang, C. Xu, H. Lin, G. Liu, J. Luan, A. Tian and J. Zhang, *Inorg. Chem. Commun.,* 2012, **24**, 43-46; (e) Y. Wang, L. Ye, T.-g. Wang, X.-B. Cui, S.-Y. Shi, G.-W. Wang and J.-Q. Xu, *Dalton Trans.,* 2010, **39**, 1916-1919; (f) Z.-J. Liu, S. Yao, Z.-M. Zhang and E.-B. Wang, *RSC Adv.*, 2013, **3**, 20829-20835; (g) Y. Yang, J. Gong,
80 W. Zhang, H. Zhang, L. Zhang, Y. Liu, H. Huang, H. Hu and Z. Kang, *RSC Adv.*, 2012, **2**, 6414-6416; (h) A. Müller, C. Beugholt, P. Kögerler, H. Bögge, S. Bud'ko and M. Luban, *Inorg. Chem.*, 2000, **39**, 5176-5177.

2. (a) M. T. Pope, *Heteropoly and Isopoly Oxometalates*, Springer-
85 Verlag, Berlin, 1983; (b) D.-L. Long, E. Burkholder and L. Cronin, *Chem. Soc. Rev.*, 2007, **36**, 105-121; (c) M. Qi, K. Yu, Z. Su, C. Wang, C. Wang, B. Zhou and C. Zhu, *Inorg. Chim. Acta* , 2013, **400**, 59-66; (d)   L. Yang, P. Ma, X. Zhang, J. Niu and J. Wang, *Inorg. Chem. Commun.*, 2013, **35**, 5-8; (e)   Y. Li, Y. Wang,
90 Y. Li and E. Wang, *Inorg. Chem. Commun.*, 2009, **12**, 112-115; (f) H. An, Y. Guo, Y. Li, E. Wang, J. Lü, L. Xu and C. Hu, *Inorg. Chem. Commun.*, 2004, **7**, 521-523; (g) L. Cronin, P. Kögerler and A. Müller, *J. Solid State Chem.,* 2000, **152**, 57-67; (h) L.-J. Chen, X. He, C.-K. Xia, Q.-Z. Zhang, J.-T. Chen, W.-B. Yang and C.-Z. Lu, *Cryst.*
95 *Growth Des.*, 2006, **6**, 2076-2085; (i). P. Dong, Q.-K. Zhang, F. Wang, S.-C. Chen, X.-Y. Wu, Z.-G. Zhao and C.-Z. Lu, *Cryst. Growth Des.*, 2010, **10**, 3218-3221.

3. (a) D. Hagrman, P. J. Zapf and J. Zubieta, *Chem. Commun.*, 1998, 1283-1284; (b) D. Hagrman, R. C. Haushalter and J. Zubieta, *Chem.*
100 *Mater.*, 1998, **10**, 361-365; (c) D. J. Chesnut, D. Hagrman, P. J. Zapf, R. P. Hammond, R. LaDuca Jr, R. C. Haushalter and J. Zubieta, *Coord. Chem. Rev.*, 1999, **190–192**, 737-769.

4. D. Hagrman, C. Zubeita, D. J. Rose, J. Zubieta and R. C. Haushalter, *Angew. Chem. Int. Ed.*, 1997, **36**, 873-876.

5. S. Chakrabarti and S. Natarajan, *Cryst. Growth Des.*, 2002, **2**, 333-335.

6. (a) S. Jones, H. Liu, C. C. O'Connor and J. Zubieta, *Inorg. Chem. Commun.*, 2010, **13**, 412-416; (b) M. Bartholomae, S. Jones and J. Zubieta, *Inorg. Chem. Commun.*, 2011, **14**, 107-110; (c) L.-J. Chen, X. He, C.-K. Xia, Q.-Z. Zhang, J.-T. Chen, W.-B. Yang and C.-Z. Lu, *Cryst. Growth Des.*, 2006, **6**, 2076-2085; (d) J. Gu, X. Jiang, Z. Su, Z. Zhao and B. Zhou, *Inorg. Chim. Acta* , 2013, **400**, 210-214; (e) C.-h. Tian, Z.-g. Sun, J. Li, X.-f. Zheng, H.-d. Liang, L.-c. Zhang, W.-s. You and Z.-m. Zhu, *Inorg. Chem. Commun.*, 2007, **10**, 757-761.

7. (a) M.-X. Li, H.-L. Chen, J.-P. Geng, X. He, M. Shao, S.-R. Zhu and Z.-X. Wang, *CrystEngComm*, 2011, **13**, 1687-1692; (b) M. Sarma, T. Chatterjee and S. K. Das, *J. Mol. Struct.*, 2011, **1004**, 31-38.

8. M.-X. Yang, S. Lin, L.-J. Chen, X.-F. Zhang and H. Huang, *Inorg. Chem. Commun.*, 2011, **14**, 1652-1655.

9. X.-Y. Wu, Q.-G. Zhai, L.-J. Chen, W.-B. Yang and C.-Z. Lu, *Chin. J. Struct. Chem.*, 2007, **26**, 389-394.

10. (a) P. Dong, Q.-K. Zhang, F. Wang, S.-C. Chen, X.-Y. Wu, Z.-G. Zhao and C.-Z. Lu, *Cryst. Growth Des.*, 2010, **10**, 3218-3221; (b) Y. Zhang, P. J. Zapf, L. M. Meyer, R. C. Haushalter and J. Zubieta, *Inorg. Chem.*, 1997, **36**, 2159-2165.

11. (a) H. Kraus and R. Prins, *J. Catal.*, 1996, **164**, 251-259; (b) C. Yin, L. Zhao, Z. Bai, H. Liu, Y. Liu and C. Liu, *Fuel*, 2013, **107**, 873-878.

12. $Ni_2(4,4'-bpy)Mo_4(4,4'-bpy)_2O_{14}$ (**1**). A mixture of $(NH_4)_6Mo_7O_{24}$ (0.374 g, 0.3 mmol), $Ni(NO_3)_2$ (0.145 g, 0.05 mmol), and 4,4'-bpy (0.165 g, 1.06 mmol) and H_2O (30 mL, 1667 mmol) was stirred and the pH value was adjusted to 5.8. The resulting suspension was sealed in a 50 mL Teflon lined reactor and kept at 140 ℃ for 3 days. After cooling the autoclave to room temperature, green block crystals were obtained (yield: 38% based on Mo). Elemental analysis for $C_{30}H_{24}Mo_4N_6Ni_2O_{14}$ calcd (%): C, 30.16; H, 2.01; N, 7.04; Ni, 9.83; Mo, 32.15. found: C, 29.66; H, 1.72; N, 7.07; Ni, 9.72; Mo, 32.11. IR (KBr, cm^{-1}): 3440 (w), 1637 (m), 1609 (m), 1554 (w), 1532 (w), 1516 (w), 1488 (s), 1410 (s), 1356 (w), 1335 (w), 1322 (w), 1218 (s), 1079 (s), 1049 (s), 944 (m), 869 (w), 800 (w), 943 (w), 863 (w), and 779 (w).

13. M. H. Chisholm, F. A. Cotton, M. W. Extine and R. L. Kelly, *J. Am. Chem. Soc*., 1978, **100**, 3354-3358.

14. W. B. Cross, J. C. Anderson, C. Wilson and A. J. Blake, *Inorg. Chem.*, 2006, **45**, 4556-4561.

15. I. D. Brown and D. Altermatt, *Acta Crystallogr., Sect. B*, 1985, **41**, 244-247.

16. Y. Shen, J. Peng, H. Zhang, X. Yu and A. M. Bond, *Inorg. Chem.*, 2012, **51**, 5146-5151.

17. C. Janiak, *J. Chem. Soc., Dalton Trans.,* 2000, **0**, 3885-3896.

18. H. Liu, C. J. Gómez-García, J. Peng, J. Sha, L. Wang and Y. Yan, *Inorg. Chim. Acta*, 2009, **362**, 1957-1962.

19. T. E. Klimova, D. Valencia, J. A. Mendoza-Nieto and P. Hernández-Hipólito, *J. Catal.*, 2013, **304**, 29-46

20. M. Egorova and R. Prins, *J. Catal.*, 2004, **225**, 417-427..